

PartComposer: Learning and Composing Part-Level Concepts from Single-Image Examples

JUNYU LIU, Brown University, USA

R. KENNY JONES, Brown University, USA

DANIEL RITCHIE, Brown University, USA



Fig. 1. Given one-shot images that contains multiple fine-grained parts, our pipeline can learn descriptive concepts for these parts with disentanglement and flexibly re-compose them to generate new objects, for both intra-category and cross-category objects.

We present PartComposer: a framework for part-level concept learning from single-image examples that enables text-to-image diffusion models to compose novel objects from meaningful components. Existing methods either struggle with effectively learning fine-grained concepts or require a large dataset as input. We propose a dynamic data synthesis pipeline generating diverse part compositions to address one-shot data scarcity. Most importantly, we propose to maximize the mutual information between denoised latents and structured concept codes via a concept predictor, enabling direct regulation on concept disentanglement and re-composition supervision. Our method achieves strong disentanglement and controllable composition, outperforming subject and part-level baselines when mixing concepts from the same, or different, object categories.

CCS Concepts: • **Computing methodologies** → **Machine learning**; **Computer graphics**.

Additional Key Words and Phrases: personalization, multiple visual concept extraction, information theory, example-based modeling

1 Introduction

Visually inspired and creative generation emerges from the ability to compose new objects from familiar parts [19, 20]. From virtual creatures to fantastical designs, part-level concept composition is a powerful paradigm for visual imagination. For instance, given images of several example chairs (Figure 1), designers could imagine composing a new chair that contains parts borrowed across the

example chairs and is structurally realistic. However, there are two major challenges for this task. Firstly, the **part-level** concepts are more fine-grained than subject-level concepts, and require structural information to be composed into reasonable objects. This makes it more challenging to properly learn the identity of concepts and achieve clear disentanglement between different concepts. Secondly, without dedicated 3D models or multi-view images of objects, most real-world examples in concept learning and composition are **single-image examples** (i.e., there is just one image per object). Such scarce data results in very poor data variety (i.e., very limited ground truth part composition), challenging the capability of generative models to properly compose unseen combinations.

A commonly used approach in concept learning is to extract visual concepts from generative models in the form of latent codes [6, 8, 12, 15, 22, 23, 25]. Each of the extracted concepts encodes the identity of an image object (e.g., a red seat cushion) and can be used with other concepts in creative image generation [2, 11, 16, 19]. In this context, text-to-image diffusion models serve as a versatile tool for learning compositional concepts through personalization. A common paradigm is to learn new or specialized token embeddings for concepts, through finetuning the diffusion model (updating the embeddings and/or the model weights) via latent diffusion loss. The learned concepts token embeddings can be directly used in prompts at inference time to generate images containing the target concepts. Several recent methods have explored dealing with single-image inputs [2, 7, 12, 23, 25], but they operate at the *subject level*. Other methods focus on part-level concept learning [16, 20], but they

Authors' Contact Information: Junyu Liu, Brown University, Providence, USA, ljuniu381@gmail.com; R. Kenny Jones, Brown University, Providence, USA, russel_jones@brown.edu; Daniel Ritchie, Brown University, Providence, USA, daniel_ritchie@brown.edu.

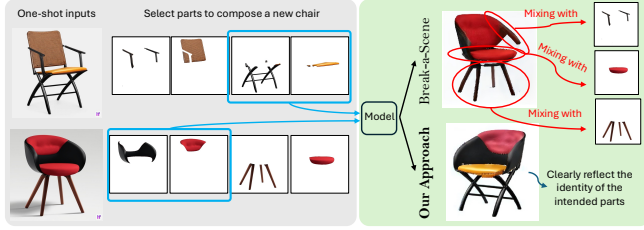


Fig. 2. Illustration of the challenge in learning fine-grained concepts from one-shot inputs. Break-a-Scene [2] results in multiple entanglement while our method cleanly reflect target concepts.

require a dataset of images as input. A common problem is that these methods tend to fail to disentangle and retain the identity of fine-grained parts. Although several works [2, 16] propose to use cross-attention loss between concept tokens and the visual contents to disentangle concepts, our experiments show that this method alone cannot effectively deal with part-level concepts from one-shot inputs. Figure 2 illustrates this problem when composing 4 parts across 2 chairs, where some part-level concepts are ambiguous or even missing in composing new part combinations.

To overcome these challenges, we make two critical observations and propose corresponding modifications. Firstly, proper augmentation on the possible part combinations should be explored and the structural integrity of objects should be preserved in the generative model prior. We propose a **dynamic data synthesis pipeline** to generate rich part-level supervision from single-image examples, by grouping union-sampled input images with randomly synthesized part combination images. Secondly, we observe that there is lack of regulation of the information encoded in different concepts, resulting in entangled and ambiguous concept learning and composition. We propose a **mutual information maximization framework** that explicitly aligns denoised latents with structured part-level concept codes, by inferring which concepts are preserved given denoised latents. To effectively formalize such regulation, we argue that penalizing both wrong compositions and wrong localization of concepts are essential to achieve good concept disentanglement. Thus, we introduce a concept predictor that performs both classification and segmentation on latent features, regularizing the embedding space to reflect concept presence and spatial structure.

We evaluate our methods on single-image part composition tasks from same object categories and across different categories. We compare the part composition results with several baselines [2, 11, 16, 20] in terms of concept preserving capability and visual quality. Our method significantly out-performs baselines in preserving correct identity of intended part-level concepts, while maintaining image quality. When given cross-category examples, our methods can produce interesting part composition of virtual objects with reasonable structure (Figure 1), enabling great artistic imagination. We also provide an ablation study for our key designs and demonstrate the flexibility of our methods on different input forms.

In summary, our contributions are: (1) We propose to focus on a challenging task, learning part-level concepts from single-image inputs, that relaxes input requirement and can be directly applied

on most real-world images. (2) We propose a dynamic data synthesis pipeline to automatically augment the scarce one-shot inputs and balance between structural integrity and part combination variety. (3) We propose a maximizing information scheme to explicitly disentangle the information encoded in concepts and supervise composition through a concept predictor with classification and segmentation.

2 Background in Visual Concept Learning

Input Requirements. Pioneering works like Textural Inversion [6] and DreamBooth [22] in visual concept learning require multiple images as input to encode a single a concept. Several follow-up works have loosen the input constraint as learning single concept from single-image examples [12, 23, 25]. Multi-concept learning from multiple inputs are also being discovered [8, 15]. Break-a-Scene [2] first propose a pipeline to learn multiple subject-level concepts from single images, enabling great flexibility in learning and remixing concepts from general use cases.

Concept Granularity. Most concept learning methods focus on learning concept for the entire image or on the subject level [2, 7–9, 11–13, 15, 23, 25]. The target use case for these methods is to generate images that are organically composed by required subject(s) according to user-specified prompts. However, to enable more creativity in generating new subjects, part-level concept learning is required. This more fined-grained concept learning task has been explored by PartCraft [16]. They learn a large dictionary of concepts for different parts of creatures and generate new virtual creatures that have not been seen in the real world. However, their method rely on training on a large dataset and struggle on single-image examples. Piece-it-Together (PiT) [20] also targets part-level concept learning, by directly operating in a carefully chosen IP-Adapter+ [27] representation space and synthesizes a complete and coherent concept by training a generative model to fill in missing information conditioned on a strong domain-specific prior. Unlike optimization-heavy approaches, PiT enables efficient inference, supports diverse sampling from sparse inputs, and allows flexible semantic manipulation. However, PiT requires training on class-specific datasets, where single-image examples are not supported and generalization to out-of-distribution data is limited.

Common Challenges. A common challenge in multi-concept learning is to disentangle the identity of concepts [2, 11, 16]. To achieve good disentanglement, dynamic masking different compositions of concepts and using cross-attention mechanisms to regulate the diffusion model finetuning are commonly used in methods like Break-a-Scene [2] and PartCraft [16]. MuDI [11] proposes a dynamic concept composition method and mean-shifted inference technique to further improve the decoupling of different concepts. However, concepts missing or inaccurate identity still occur in all of these methods when re-composing concepts in generative process [2, 11, 16], especially when dealing with 4 or more concepts. Our observation is that all existing concept learning works do not provide any explicit regulation on the information encoded in different concepts and the composition process, causing inaccurate

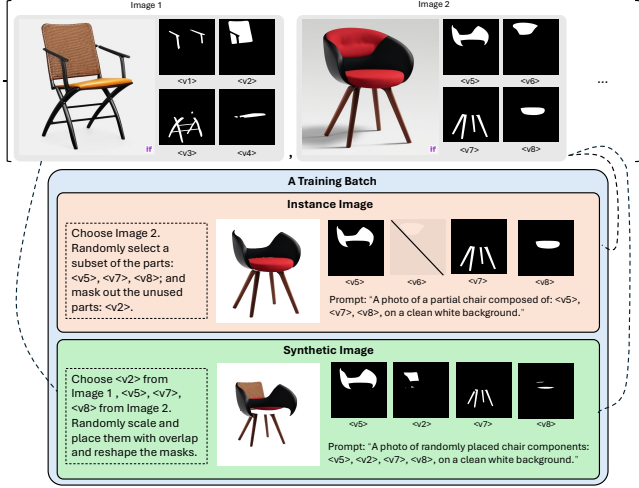


Fig. 3. Dynamic data synthesis. Each training batch includes an instance image with masked parts and a synthetic image with randomly sampled and placed parts from multiple inputs, enabling diverse part-level supervision from single-image examples.

multi-concept remixing. Other common challenges include learning large number of concepts (e.g., more than 4) from single inputs [2].

3 Method

Given single-image examples, we want to be able to learn part concepts and re-compose them from each input together arbitrarily. Our pipeline build upon the commonly used diffusion model customization approaches (introduced in Section 1) like Break-a-Scene [2] and PartCraft [16], where standard diffusion loss \mathcal{L}_{ldm} and cross-attention losses $\mathcal{L}_{\text{attn}}$ are used to learn and disentangle concept tokens. However, to enable learning concepts at part level with single-image examples, we propose a dynamic data synthesis method to augment the limited data and a maximizing mutual information scheme to enable clear disentanglement of parts' concepts and good composition capabilities for the generative model. Figure 4 gives an overview of our approach.

We want to highlight that although our pipeline is built on text-to-image diffusion models, we treat part-level concepts as purely visual information and do not require semantic or annotations for the part concepts. The tokens and text prompts only serve as media of templates to encode and convey such information.

Dynamic Data Synthesis. We propose a dynamic data synthesis approach to augment the limited single-image example input. Our goal is to explore and augment part combination variety while preserving structural integrity information in the diffusion prior. We formalize the training batch from the given examples and a synthetic image that is generated on-the-fly. Figure 3 demonstrates our dynamic data synthesis approach. To preserve the structural information of the diffusion prior, the instance image is randomly chosen from the input examples, since they contain reasonable object structures. We randomly select a subset of the parts contained in the chosen

instance image, inspired by the union sampling method in Break-a-Scene [2]. We mask out the unused parts areas and change the background to white to focus only on the part concepts, and pair it with a descriptive prompt. However, this data alone cannot provide enough training data to finetune diffusion models to compose different compositions of parts across different images. Thus, to explore and augment part combination variety, we propose to synthesize an image that contains parts that are randomly sampled across input examples. For each part category (e.g., the armrest of the chair), we randomly select a part from the input instances. Inspired by MuDI [11], we randomly scale and place the sampled parts on an white image. The parts can overlap each other to encourage learning concepts from multiple possible compositions. We modify the original masks according to the overlapping occlusions. Due to the high variability in the synthetic image, we use a different prompt to treat it as a collection of parts. Additional dynamic data synthesis explanation and examples can be found in Appendix A.

Maximizing Mutual Information. Most existing concept learning methods either rely on multiple inputs [8, 15, 16] or are restricted by the number of concepts they could learn at the same time [12, 23, 25]. These restrictions results in poor performance in applying them on learning part-level concepts. We argue that a key missing point is that there are no explicit regulation on the information encoded in the concept embeddings and the composition process of the generative model. We thus propose a scheme to maximize the mutual information between the denoised latents and the concepts contained in the input image, and thus disentangle the information encoded in each part-level concepts and supervise the diffusion generative process.

To this end, we adopt a mutual information maximization objective inspired by InfoGAN [4], which encourages the learned concept embeddings to retain interpretable and disentangled semantic structure. Let \tilde{z} denote the denoised latent representation, and let c denote the set of concept codes associated with the input image. We seek to maximize the mutual information $I(c; \tilde{z})$, which quantifies how much information about the concepts is preserved in the latent. This can be expressed as:

$$I(c; \tilde{z}) = H(c) - H(c | \tilde{z}),$$

where $H(c)$ is the entropy of the concept distribution and $H(c | \tilde{z})$ is the conditional entropy of the concepts given the latent. Since directly computing this term is intractable, we introduce a variational distribution $Q(c | \tilde{z})$, implemented via a neural network - concept predictor, to approximate the true posterior. This leads to a variational lower bound:

$$\mathcal{I}_{\text{lower}} = \mathbb{E}_{c \sim P(c), \tilde{z} \sim P(\tilde{z}|c)} [\log Q(c | \tilde{z})] + H(c),$$

which satisfies $\mathcal{I}_{\text{lower}} \leq I(c; \tilde{z})$. For a fixed prior over concepts (i.e., the ground-truth labels that supervise the concept predictor), $H(c)$ is constant and can be omitted during optimization. The corresponding training loss $\mathcal{L}_{\text{Info}}$ is defined as the negative of the lower bound :

$$\mathcal{L}_{\text{Info}} = -\mathbb{E}_{c \sim P(c), \tilde{z} \sim P(\tilde{z}|c)} [\log Q(c | \tilde{z})],$$

which is minimized alongside the task loss. This encourages the model to produce latents \tilde{z} from which the concept codes c can be accurately inferred, effectively regularizing the concept embedding

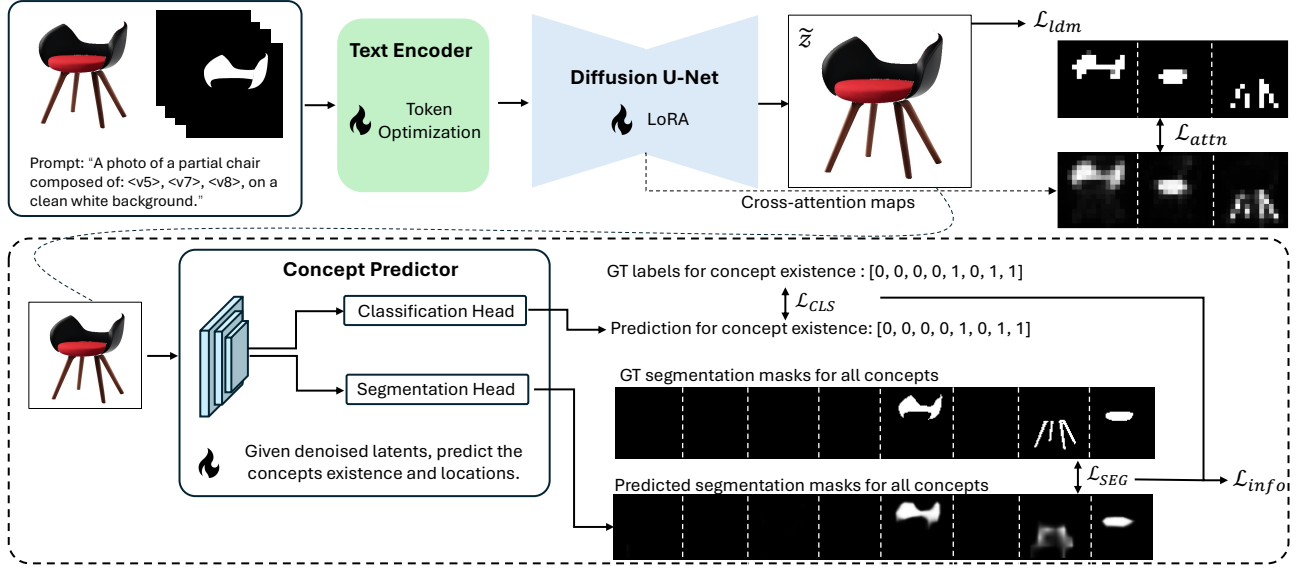


Fig. 4. Overview of our method. Given a concept-compositional prompt and noise input, the denoising U-Net produces a latent \tilde{z} supervised by reconstruction loss \mathcal{L}_{ldm} , cross-attention losses \mathcal{L}_{attn} , and information loss \mathcal{L}_{info} . \mathcal{L}_{info} is computed by a concept predictor which receives \tilde{z} and outputs concept classification and segmentation logits. The goal is to maximize mutual information between latent features and concept codes. All modules are jointly optimized to enable part-level concept disentanglement and controllable composition.

space to reflect correct part-level visual information. This framework provides direct supervision to disentangle part-level concepts and penalizes the generative models from generating ambiguous or missing part combinations.

To effectively implement a $Q(c | \tilde{z})$, we propose the concept predictor design as shown in Figure 4, which includes two output heads to provide both classification and segmentation predictions of concepts given an denoised latent. The classification loss \mathcal{L}_{CLS} penalizes the wrong compositions of concepts (i.e., missing concepts or containing more concepts). The segmentation loss \mathcal{L}_{SEG} further penalizes wrong localization of concepts (i.e., wrong or entangled location of concepts). An visualized example of the ground truth localization masks and predicted localization segmentation are shown in Figure 4. We also provide visualization for convergence of the segmentation head throughout the training steps in Appendix D. These two losses are weighted to have the same scale and combined to get the mutual information loss \mathcal{L}_{Info} . The concept predictor is jointly optimized with the concept learning process.

Overall pipeline. Our overall training loss consists the latent diffusion loss \mathcal{L}_{ldm} and cross-attention loss \mathcal{L}_{attn} from the original Break-a-Scene pipeline, with our concept prediction loss composed by the classification loss \mathcal{L}_{CLS} and segmentation loss \mathcal{L}_{SEG} . We also use an auxiliary background loss \mathcal{L}_{BG} to further improve the generated image quality, which penalizes generation of content outside the union of selected part masks. This encourages the model to focus on concept-relevant regions and avoid unrelated artifacts in unmasked areas. Thus, the total loss is defined as: $\mathcal{L}_{total} = \mathcal{L}_{ldm} + \mathcal{L}_{attn} + \lambda_{info}(\mathcal{L}_{CLS} + \lambda_{seg}\mathcal{L}_{SEG}) + \lambda_{bg}\mathcal{L}_{BG}$, with the following loss weights: $\lambda_{info} = 0.05$, $\lambda_{seg} = 10.0$, $\lambda_{bg} = 0.01$.

4 Experiments

In this section, we first introduce our experiment setup in terms of data and mask generation, implementation details, and comparison details. We then show the qualitative results and comparisons followed by quantitative evaluations.

4.1 Experiments Setup

Data and Mask Generation. We use both synthetic data and real-world images in our experiments. We generate the synthetic images using DeepFloyd IF [5] and we collect real-world images mainly from renderings of 3D objects [18].

Our method assumes access to part-level masks for training, but remains agnostic to how these masks are obtained. In practice, we adopt one of the following strategies depending on the dataset:

- **Automatic segmentation and labeling:** We apply off-the-shelf segmentation models such as SAM [14] to produce over-segmented masks, followed by GPT-4o-based [1] captioning and labeling to group and assign part identities.
- **Manual or direct annotation:** We directly specify or provide part masks, either manually or from existing annotated assets (e.g., 3D renderings [18] or synthetic data).

Our framework is compatible with any source of part-level supervision, including both automatic and manual pipelines. Since the main focus of our work is not on the mask generation itself, we treat this step as a pre-processing module and do not over-emphasize our effort on it.

Implementation Details. For all experiments, we use Stable Diffusion v2.1 [21] as the pre-trained text-to-image diffusion model and apply LoRA [10] with rank 32 to the U-Net module. The concept

predictor is a convolutional network that operates on denoised latents and outputs both classification and segmentation predictions. It consists of three convolution layers (with output channels 16, 32, and 64), followed by two parallel output heads: a classification head composed of two fully connected layers for predicting multi-label concept presence, and a segmentation head consisting of a 1×1 convolution followed by bilinear upsampling to produce per-concept spatial masks. We follow a two-stage training scheme similar to Break-a-Scene [2], where we only update the token embeddings with a high learning rate (10^{-4}) in the first stage and fully update both text encoder and LoRA weights in the U-Net with a low learning rate (10^{-6}) in the second stage. More training and inference details are introduced in Appendix A.

Comparison Details. For finetune-based approaches in concept learning, we compare our methods with 3 representative methods: Break-a-Scene [2], which is representative for concept learning from a single image, PartCraft [16], which is representative for part-level concept learning from large datasets, and MuDI [11], which is representative for disentangling subject-level concepts. To align their setting with our task, we adapt the original Break-a-Scene input dataset into a single-image examples input manner and feed part-decomposed examples into PartCraft and MuDI pipeline. We also conduct comparison with PiT [20], which train dedicated priors for different categories and encode and recompose part-level concepts at test time. We directly use their provided checkpoints and prepare corresponding examples to inference and compare with our results. More implementation details for the adaptation of their methods are explained in Appendix B.

4.2 Results

4.2.1 Qualitative Evaluation. We provide qualitative evaluation and comparisons our pipeline with other methods. We use two tasks - intra-category and cross-category inputs, each with more than 5 distinctive examples, to demonstrate the effectiveness of our pipeline in part-level concept learning and mixing.

Intra-category Results. We first demonstrate the part-level concept learning and composition capability of our model using inputs from same categories. The input subjects consist same part decompositions (e.g., we decompose a chair into 4 parts: armrest, seat back, legs, and seat in Figure 5.) Note that we do not require the part decompositions to be semantically meaningful since our method can handle any part-level visual concepts.

Figure 5 shows the qualitative comparison of our method with Break-a-Scene [2], PartCraft [16], and MuDI [11], where we aim to recompose concepts across two input images. We generate 4 samples for each part composition. Break-a-Scene [2] struggles to disentangle and recompose part-level concepts, resulting in mixed identity in different parts, presumably since it was designed to do subject-level concept learning. PartCraft struggles to learn and recompose part-level concepts from single-image examples, resulting in poor and inconsistent image generation quality, presumably since it was designed to train on a large dataset. MuDI struggles to learn effective part-level concepts and result in poor composition capability, presumably since it was designed for few subject-level

concepts disentanglement. Our pipeline produce clear part-level concept disentanglement and clean composition capability.

To enable fair comparison with PiT [20] on their pre-trained checkpoints, we conduct two experiments, one for in-distribution and one for out-of-distribution. We first use their training data for "creature" category and compare our results with the results generated by PiT's "creature" checkpoint. We then use a chair example to compare our results with the results generated by their "product" checkpoint, which is the closest related category in their provided checkpoints. Figure 6 illustrates the qualitative comparison results. Even for in-distribution examples (the "creature" example which is directly from their training data), PiT may drastically alter the identity of some concepts while our method generally preserves decent concept identity. When using out-of-distribution data like chairs, their pipeline fail to encode and compose provided parts.

Figure 8 illustrates the results for 2 different levels of part granularity. It demonstrates that our method is agnostic to the granularity of parts and can effectively learn a large amount of (more than the 4 parts per image) very fine-grained concepts from single-image examples. We also provide substantial additional results for over 10 different categories in Appendix C.1.

Cross-category Results. To enable more creativity in part-level concepts composition, we evaluate our methods in learning and composing parts from objects in different categories, aiming to generate virtual objects. The first row in Figure 5 shows hybrid compositions from a wheelchair and a bed and the second row in Figure 5 shows hybrid compositions from a wheel chair and a chair. Our methods can generate creative virtual objects with different part compositions, preserving clear part-level identity with reasonable structural arrangements for most composition scenarios. More results are shown in Figure 1 and in appendix C.2.

4.2.2 Quantitative Evaluation. We quantitatively compare our pipeline with baselines in terms of concept preserving capability and overall image generation quality. We run experiments for 3 categories (chair, vehicle, and characters), each with 7 single-image examples, and take the averaged score. For a single-image example containing m images and with k part decomposition, we sample 36 images for each of the m^k possible part combinations, resulting in a total of around 1k image samples per example.

Concept Preserving. Our goal is to evaluate whether the intended part-level concepts are preserved in the generated images. Several previous works [2, 11] that focus on subject-level concept learning use detectors to locate the subject and then compare feature-wise distance (e.g., DINO [3]) on the located areas. However, automatically detecting fine-grained parts from subjects is hard and DINO feature comparison is not effective on parts that are small or thin. Thus, we follow the evaluation methods used in PiT [20], which use a multi-modal LLM - QWen [26] to compare the generated images with intended parts and score the visual alignment. Given k parts to compose a subject, we prompt QWen to score from 0 to k , indicating how many parts are preserved in a generated image. We then normalize the scores for all of the examples into a 0-5 scale and report in Table 4.2.2. Our method significantly outperforms baselines to preserve the most intended part-level concepts.

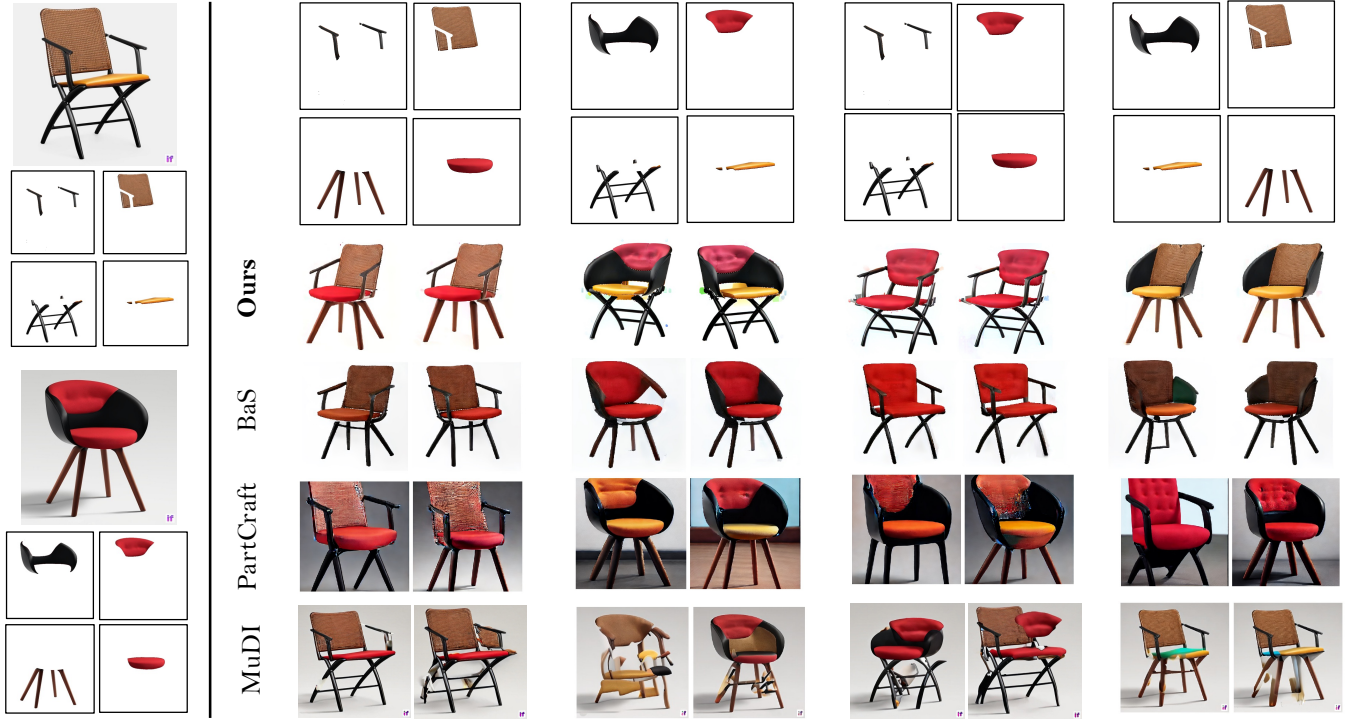


Fig. 5. Comparison of concept composition results for 2 chairs using our approach, Break-a-Scene (BaS) [2], PartCraft [16], and MuDI [11]. The input images and correspond part decompositions are shown in the left column. We illustrates 4 part composition across the two input images by selecting 2 parts from each image, which are shown on the top row. We show 2 random samples for each composition.

Category	BaS	PartCraft	MuDI	PiT	PartComposer
Chairs	3.66	1.89	1.97	2.70	4.91
Characters	4.10	3.20	2.70	4.30	4.89
Vehicles	3.07	1.85	2.03	2.57	4.68

Table 1. Concept preserving comparison. Higher is better (↑).

Generation Quality. We evaluate the overall image quality for the generated images, using 2 metrics to evaluate both the overall samples quality and single image comparison quality. We use FID and KID score to evaluate the image quality by comparing the sampled images for all possible part combinations and reference image datasets for corresponding category. For KID, we randomly divide the samples into 20 batches. The reference images are generated using SDXL [17]. We also use multi-model LLMs to evaluate the generated image quality by directly comparing the samples with the given example images. We use QWen to score the quality on a 1-5 scale on the 5 methods for each example, where the best quality method get score 5 and the worst quality method gets score 1. Table 2 shows the results. Our model generally achieves the best image quality when comparing to other models.

4.2.3 Flexibility and Scalability. We demonstrate the flexibility and scalability of our pipeline in 3 aspects: encoding background concepts together with part-level concepts, dealing with incomplete part combination prompts, and scaling to learn large number of concepts from more than 2 single-image examples. The left column

Category	Metrics	BaS	PartCraft	MuDI	PiT	PartComposer
Chair	FID ↓	17.22	26.91	16.07	23.95	15.85
	KID - Mean ↓	0.0632	0.1098	0.0551	0.0800	0.0502
	KID - Std Dev ↓	0.0066	0.0097	0.0064	0.0085	0.0067
	QWen Score ↑	2.87	1.48	3.72	2.21	4.72
Vehicle	FID ↓	20.54	18.78	22.26	20.12	18.30
	KID - Mean ↓	0.2066	0.1751	0.2342	0.1772	0.1530
	KID - Std Dev ↓	0.0093	0.0092	0.0113	0.0092	0.0095
	QWen Score ↑	2.75	1.54	3.94	2.13	4.64
Creature	FID ↓	19.26	20.87	25.06	17.56	17.26
	KID - Mean ↓	0.1314	0.1692	0.2038	0.1179	0.1018
	KID - Std Dev ↓	0.0065	0.0098	0.0071	0.0066	0.0067
	QWen Score ↑	3.10	1.64	1.60	3.98	4.68

Table 2. Generation quality comparison for 3 categories.

in Figure 9 demonstrates that our pipeline can learn background concepts with part concepts and naturally place the composed object in the background. The right column in Figure 9 shows that our method can generate structural complete objects given incomplete part combinations and can have variety in unspecified parts. The last row in Figure 10 demonstrates that our method can directly learn large number of concepts (i.e., 16 concepts from 4 single-image examples). All previous works often struggle to learn over 5 concepts at the same time without using large datasets.

4.2.4 Ablation Study and Analysis. We conduct ablation study by removing the dynamic data synthesis method and the concept predictor. Figure 7 illustrates the ablation results. Disabling the dynamic

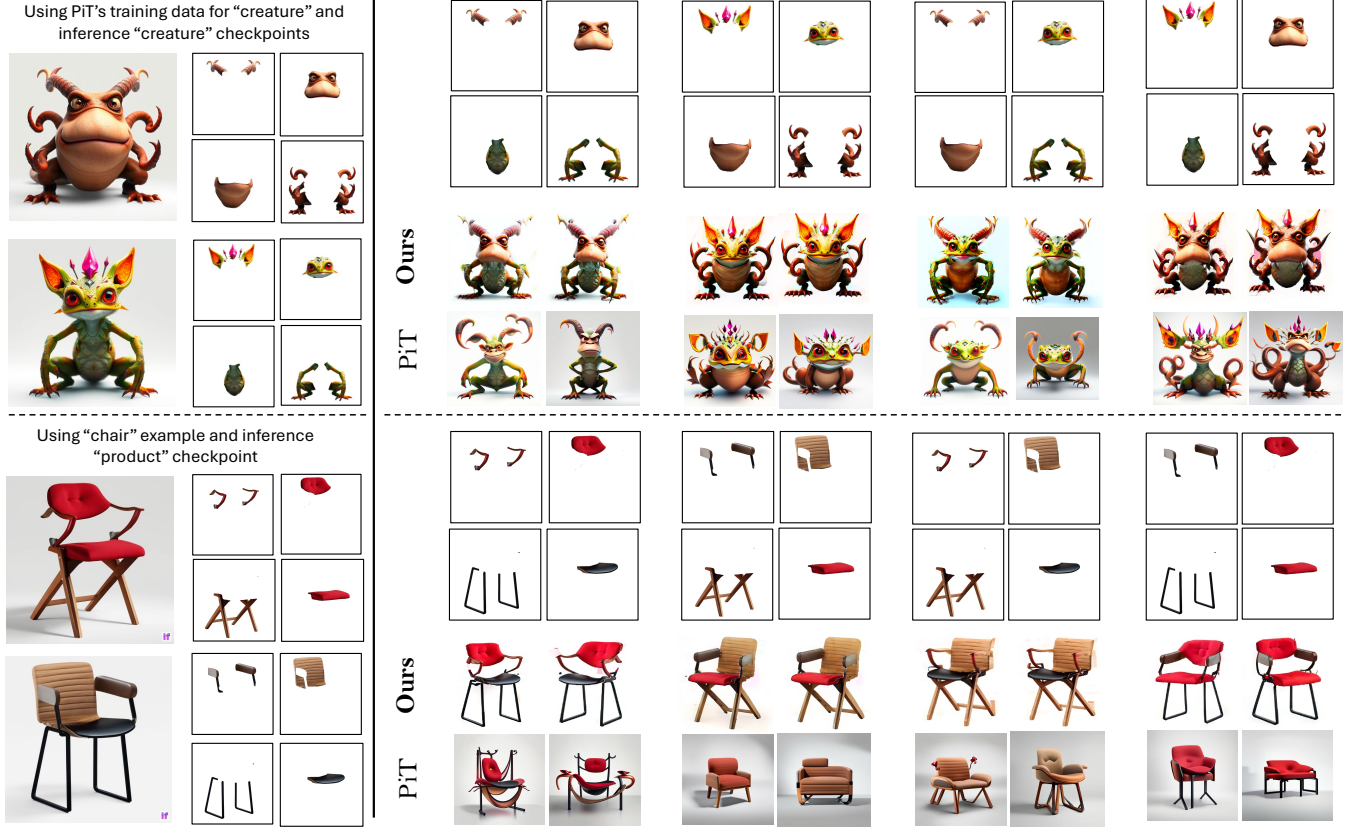


Fig. 6. Comparison of concept composition results for 2 creatures and 2 chairs using our approach and PiT [20].

data synthesis results in poor data utility and disabling the concept predictor results in concept disentanglement or missing. We also conduct visualization for the convergence of concept predictor and weight/scale experiments in Appendix D. We analyze the limitations of our method in Appendix E.

5 Conclusion

We have introduced PartComposer, a method for fine-grained concept learning that enables new visual generation capabilities through part-level combination and composition. We propose a mutual information maximization framework that guides text-to-image diffusion model customization pipelines to both disentangle input concepts and reduce 'missing concept' failure modes. Combined with a dynamic data synthesis procedure, PartComposer is able to learn how to disentangle and compose fine-grained part-level concepts from single-image examples. We found that our approach was able to produce natural part compositions, that preserved concept identity, given single-image examples, from both matching and distinct categories. One promising direction for future work would be to convert our 2D productions into fully realized 3D models, using inverse rendering or image-to-3D pipelines. Looking forward, we believe our method can benefit creative design and imagination workflows, producing novel ideations from easy to source inputs, that might help spark new inspiration and creations.



Fig. 7. Qualitative comparison across ablations: without dynamic data synthesis (w/o D.S.), without concept predictor (w/o C.P.), and our full approach.

References

- [1] Josh Achiam, Steven Adler, Sandhini Agarwal, Lama Ahmad, Ilge Akkaya, Florencia Leoni Aleman, Diogo Almeida, Janko Altschmidt, Sam Altman, Shyamal Anadkat, et al. 2023. Gpt-4 technical report. *arXiv preprint arXiv:2303.08774* (2023).
- [2] Omri Avrahami, Kfir Aberman, Ohad Fried, Daniel Cohen-Or, and Dani Lischinski. 2023. Break-a-scene: Extracting multiple concepts from a single image. In *SIGGRAPH Asia 2023 Conference Papers*. 1–12.
- [3] Mathilde Caron, Hugo Touvron, Ishan Misra, Hervé Jégou, Julien Mairal, Piotr Bojanowski, and Armand Joulin. 2021. Emerging properties in self-supervised vision transformers. In *Proceedings of the IEEE/CVF international conference on computer vision*. 9650–9660.
- [4] Xi Chen, Yan Duan, Rein Houthoofd, John Schulman, Ilya Sutskever, and Pieter Abbeel. 2016. Infogan: Interpretable representation learning by information maximizing generative adversarial nets. *Advances in neural information processing systems* 29 (2016).
- [5] DeepFloydAI. 2023. DeepFloyd IF. https://huggingface.co/docs/diffusers/api/pipelines/deepfloyd_if
- [6] Rinon Gal, Yuval Alaluf, Yuval Atzmon, Or Patashnik, Amit H Bermano, Gal Chechik, and Daniel Cohen-Or. 2022. An image is worth one word: Personalizing text-to-image generation using textual inversion. *arXiv preprint arXiv:2208.01618* (2022).
- [7] Daniel Garibi, Shahar Yadin, Roni Paiss, Omer Tov, Shiran Zada, Ariel Ephrat, Tomer Michaeli, Inbar Mosseri, and Tali Dekel. 2025. TokenVerse: Versatile Multi-concept Personalization in Token Modulation Space. *arXiv preprint arXiv:2501.12224* (2025).
- [8] Ligong Han, Yinxiao Li, Han Zhang, Peyman Milanfar, Dimitris Metaxas, and Feng Yang. 2023. Svdif: Compact parameter space for diffusion fine-tuning. In *Proceedings of the IEEE/CVF International Conference on Computer Vision*. 7323–7334.
- [9] Shaozhe Hao, Kai Han, Zhengyao Lv, Shihao Zhao, and Kwan-Yee K Wong. 2024. ConceptExpress: Harnessing diffusion models for single-image unsupervised concept extraction. In *European Conference on Computer Vision*. Springer, 215–233.
- [10] Edward J Hu, Yelong Shen, Phillip Wallis, Zeyuan Allen-Zhu, Yuanzhi Li, Shean Wang, Lu Wang, Weizhu Chen, et al. 2022. Lora: Low-rank adaptation of large language models. *ICLR* 1, 2 (2022), 3.
- [11] Sangwon Jang, Jaehyeong Jo, Kimin Lee, and Sung Ju Hwang. 2024. Identity decoupling for multi-subject personalization of text-to-image models. *arXiv preprint arXiv:2404.04243* (2024).
- [12] Xuhui Jia, Yang Zhao, Kelvin CK Chan, Yandong Li, Han Zhang, Boqing Gong, Tingbo Hou, Huisheng Wang, and Yu-Chuan Su. 2023. Taming encoder for zero fine-tuning image customization with text-to-image diffusion models. *arXiv preprint arXiv:2304.02642* (2023).
- [13] Chen Jin, Ryutaro Tanno, Amrutha Saseendran, Tom Diethe, and Philip Alexander Teare. 2024. An Image is Worth Multiple Words: Discovering Object Level Concepts using Multi-Concept Prompt Learning. In *Forty-first International Conference on Machine Learning*.
- [14] Alexander Kirillov, Eric Mintun, Nikhila Ravi, Hanzi Mao, Chloe Rolland, Laura Gustafson, Tete Xiao, Spencer Whitehead, Alexander C Berg, Wan-Yen Lo, et al. 2023. Segment anything. In *Proceedings of the IEEE/CVF international conference on computer vision*. 4015–4026.
- [15] Nupur Kumari, Bingliang Zhang, Richard Zhang, Eli Shechtman, and Jun-Yan Zhu. 2023. Multi-concept customization of text-to-image diffusion. In *Proceedings of the IEEE/CVF conference on computer vision and pattern recognition*. 1931–1941.
- [16] Kam Woh Ng, Xiatian Zhu, Yi-Zhe Song, and Tao Xiang. 2024. PartCraft: Crafting Creative Objects by Parts. In *European Conference on Computer Vision*. Springer, 420–437.
- [17] Dustin Podell, Zion English, Kyle Lacey, Andreas Blattmann, Tim Dockhorn, Jonas Müller, Joe Penna, and Robin Rombach. 2023. Sdxl: Improving latent diffusion models for high-resolution image synthesis. *arXiv preprint arXiv:2307.01952* (2023).
- [18] RenderHub. [n. d.]. RenderHub. <https://www.renderhub.com>.
- [19] Elad Richardson, Kfir Goldberg, Yuval Alaluf, and Daniel Cohen-Or. 2024. ConceptLab: Creative Concept Generation using VLM-Guided Diffusion Prior Constraints. *ACM Transactions on Graphics* 43, 3 (2024), 1–14.
- [20] Elad Richardson, Kfir Goldberg, Yuval Alaluf, and Daniel Cohen-Or. 2025. Piece it Together: Part-Based Concepting with IP-Priors. *arXiv preprint arXiv:2503.10365* (2025).
- [21] Robin Rombach, Andreas Blattmann, Dominik Lorenz, Patrick Esser, and Björn Ommer. 2022. High-Resolution Image Synthesis with Latent Diffusion Models. *arXiv:2112.10752 [cs.CV]* <https://github.com/Stability-AI/stablediffusion>.
- [22] Nataniel Ruiz, Yuanzhen Li, Varun Jampani, Yael Pritch, Michael Rubinstein, and Kfir Aberman. 2023. Dreambooth: Fine tuning text-to-image diffusion models for subject-driven generation. In *Proceedings of the IEEE/CVF conference on computer vision and pattern recognition*. 22500–22510.
- [23] Jing Shi, Wei Xiong, Zhe Lin, and Hyun Joon Jung. 2024. Instantbooth: Personalized text-to-image generation without test-time finetuning. In *Proceedings of the IEEE/CVF conference on computer vision and pattern recognition*. 8543–8552.
- [24] Jiaming Song, Chenlin Meng, and Stefano Ermon. 2020. Denoising diffusion implicit models. *arXiv preprint arXiv:2010.02502* (2020).
- [25] Yuxiang Wei, Yabo Zhang, Zhilong Ji, Jinfeng Bai, Lei Zhang, and Wangmeng Zuo. 2023. Elite: Encoding visual concepts into textual embeddings for customized text-to-image generation. In *Proceedings of the IEEE/CVF International Conference on Computer Vision*. 15943–15953.
- [26] An Yang, Anfeng Li, Baosong Yang, Beichen Zhang, Binyuan Hui, Bo Zheng, Bowen Yu, Chang Gao, Chengen Huang, Chenxu Lv, et al. 2025. Qwen3 Technical Report. *arXiv preprint arXiv:2505.09388* (2025).
- [27] Hu Ye, Jun Zhang, Sibio Liu, Xiao Han, and Wei Yang. 2023. Ip-adapter: Text compatible image prompt adapter for text-to-image diffusion models. *arXiv preprint arXiv:2308.06721* (2023).



Fig. 8. Concept learning and composition results for two virtual creatures at coarse and fine part segmentation levels. Our pipeline can effectively learn very fine-grained part-level concepts from single-image examples.

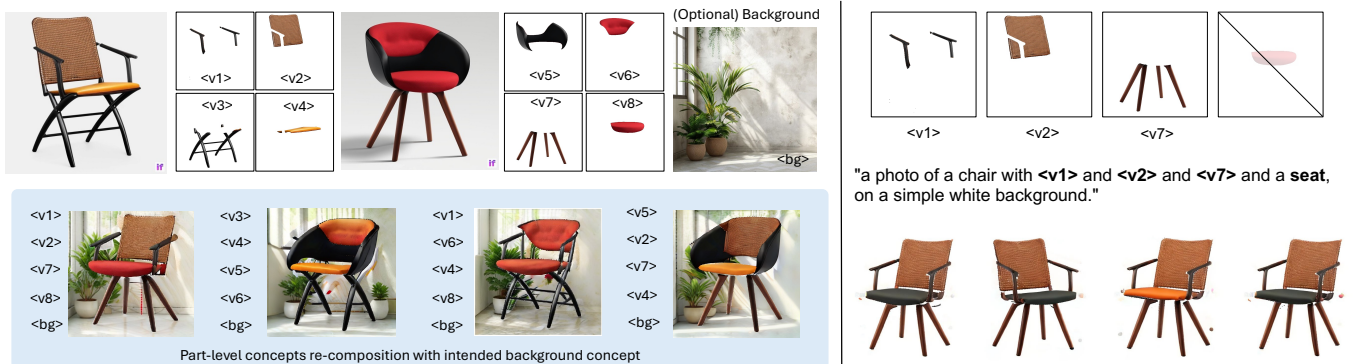


Fig. 9. Flexibility of our pipeline: Our pipeline can learn background concept together with part concepts, and naturally blend the composed objects into the background (left column). Our pipeline can also handle incomplete combination of parts in a prompt and generate complete objects with variations in the unspecified parts.

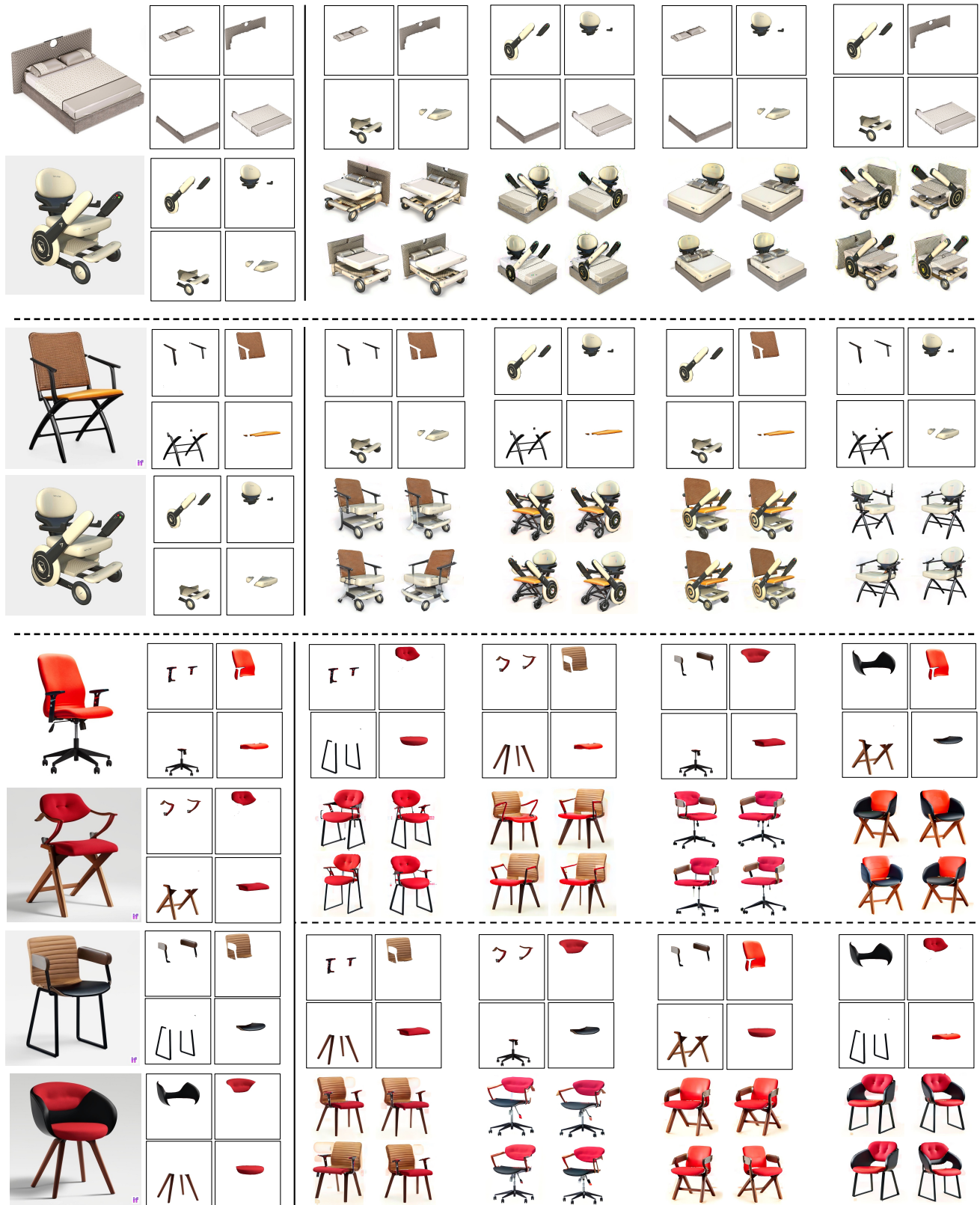


Fig. 10. Concept learning composition results for more cross-category data and scaled-up single-image examples (16 concepts at one time).

A Training Details

We provide the detailed training configuration used in our experiments for learning part-level visual concepts from single-image examples. Our pipeline is trained using Stable Diffusion v2.1 [21] as the base text-to-image model. We use a pair of chair images from Figure 3 as an illustrative example. Each chair is decomposed into four semantic parts: armrest, backrest, legs, and seat. These parts are tokenized into 8 learnable placeholder tokens, denoted as $\langle v1 \rangle$ through $\langle v8 \rangle$, with each token corresponding to a specific part instance from the two training images.

Prompt Design. Each training image is paired with a structured, part-compositional prompt using the assigned placeholder tokens. Two types of prompts are generated dynamically during training:

- **Instance prompts:** These describe partial objects composed of a subset of parts from a single input image. For example, if parts $\langle v5 \rangle$, $\langle v7 \rangle$, and $\langle v8 \rangle$ are selected from Image 2, the corresponding prompt is: “A photo of a partial chair composed of: $\langle v5 \rangle$, $\langle v7 \rangle$, $\langle v8 \rangle$, on a clean white background.”
- **Synthetic prompts:** These describe compositions of parts sampled across both input images. For example, if $\langle v2 \rangle$ is sampled from Image 1 and $\langle v5 \rangle$, $\langle v7 \rangle$, and $\langle v8 \rangle$ are sampled from Image 2, the prompt is: “A photo of randomly placed chair components: $\langle v2 \rangle$, $\langle v5 \rangle$, $\langle v7 \rangle$, $\langle v8 \rangle$, on a clean white background.”

All prompts are automatically generated based on the selected part indices. Backgrounds are set to white by default, and prompts are templated consistently to ensure clean compositional control.

Training Procedure. We adopt a two-phase training scheme:

- **Phase 1:** Only concept token embeddings are optimized for 6,400 steps.
- **Phase 2:** The LoRA-injected U-Net (with rank 32) and text encoder are jointly fine-tuned for 40,000 steps.

We want to note that the second stage training step number is just a rough reference which generally ensures that all concepts are well-learned, and removes background contents. In general, after 18,000 steps, the concept learning and re-composition results are already good enough.

Inference Procedure. We perform inference using standard DDIM [24] sampling with a pretrained Stable Diffusion v2.1 backbone, the optimized text encoder, and the learned LoRA weights. Given a compositional prompt (e.g., “A photo of a partial chair with $\langle v2 \rangle$, $\langle v5 \rangle$, $\langle v7 \rangle$, $\langle v8 \rangle$, on a clean white background.”), the model decodes a final image using 50 DDIM steps. We use a commonly used guidance scale 7.5.

Learning Extra Background Concepts. Our pipeline also supports learning extract background concepts if user wants to place the re-composed object on specific background images. We use $\langle bgX \rangle$ to represent the background concepts and they are learned together with the part-level concepts. In our data dynamic data synthesis stage, we replace the white background with the given background images and keep all other operations as the same. We use the background loss λ_{bg} with weight $\lambda_{bg} = 0.01$ to train the background concepts. Figure 9 show the results for incorporating an indoor

background with re-composed chairs. Our method can naturally blend the newly composed chair into the given background.

B Comparison Implementation

We compare our method with other visual concept learning and re-composition works, Break-a-Scene [2] and PartCraft [16]. We introduce the detailed comparison experiment setup in this section.

Break-a-Scene [2] is originally designed to learn multiple subject-level concepts in a single image. We modify the data loading and processing scheme to support learning part-level concepts from single-image examples. In addition, since we can only access 24G VRAM GPU (RTX3090), we add LoRA [10] following standard StableDiffusion v2.1 model finetuning scheme to train the LoRA weights instead of the entire diffusion U-Net. This approach has been validated by PartCraft [16] that it will not harm the concept learning quality when compared to finetuning the entire U-Net.

PartCraft [16] is originally designed to learn part-level concepts from a large dataset of images. Specifically, they require to have 10-20 images for a subject (e.g., a specific bird species.). We modify the data loading and processing scheme to load single-image examples dataset into their pipeline. In addition, we directly provide the part-level masks instead of using their automatic concept discovering method to ensure fair comparison. We use StableDiffusion v1.5 as described in their paper to learn the concepts. Their approach show unstable performance. The results we show in Figure 5 are already the best results we observed. The image quality degrades quickly when the training step number increases (after the step we shown in Figure 5). We also tried to use smaller learning rate but their pipeline struggle to even learn any meaningful concepts. We hypothesis the reason for this is that their method is designed to use on a large dataset instead of the single-image examples in our case.

MuDI [11] is originally designed to learn and disentangle similar subject-level concepts from multi-image examples. They generally require over 5 images per subject. We use the SDXL with LoRA as described in their paper to finetune the diffusion model. For the inference, we use their official inference code which first creates a mean-shifted noise by pasting intended part onto a blank image and then add noise, and then run SDXL [17] to iteratively denoise. The results we show in Figure 5 is already the best results we observed. Their approach struggle at part-level and with more than 5 concepts - the single-image example of 2 chairs contains 8 concepts.

PiT [11] is originally designed for creative visual designs by training priors for different object categories and infer creative designs given different part inputs. This method only require test-time inference, which is different with all the above methods and our methods which are optimization-based. Since we don't have access to their full training data, we directly use their released 3 checkpoints (product, creature, and toy) to conduct evaluation. To enable fair comparison, we first use 2 “creature” images that are used in their training and inference through their released “creature” checkpoint. The goal is to evaluate their concept learning and composition capability for in-distribution data. We then use 2 “chair” images and inference through their “product” checkpoint, which is the most related checkpoint in terms of category similarity. The goal for this

design is to evaluate their capability to encode and compose parts for slightly out-of-distribution examples.

C Extra Experimental Results

C.1 Intra-category Results

We conduct experiments on various object categories to demonstrate our model's capability in learning and re-composing part-level concepts. In each case, objects are decomposed into over four semantic parts, and our method learns to mix these parts across instances from the same category. We want to note that all the semantic part naming are annotated just for ease-of-read in the paper. We do not require semantically meaningful part decomposition and detailed annotation for the part-level concepts in our pipeline since we only treat them as visual information.

Chair. Parts are: armrest, backrest, legs, and seat. Figure 11 and Figure 12 show concept composition results across 6 different chair pairs.

Bed. Parts are: headboard, base, mattress, and pillow. Figure 13 shows concept composition for a pair of beds.

Gym Equipment. Parts are: base, stand, seat, and weight. Figure 14 shows concept composition for a pair of gym equipment examples.

Vehicle. Parts are: front, cockpit, tail, and wheels. Figure 15 shows concept composition for three pairs of vehicles.

Bike. Parts are: handle, frame, seat, and wheels. Figure 16 shows concept composition results for a pair of bikes.

Plane. Parts are: body, wing, tail, and engine. Figure 17 shows concept composition results for a pair of planes.

Robot. Parts are: head, body, arm, and leg. Figure 18 shows concept composition results for a pair of robots.

Bird and Dragon. Parts are: head, body, wings, tail, and legs. Figure 19 shows concept composition for a bird and a creature pair.

Virtual Characters. Figure 20 shows concept composition for a mushroom-like character and a santa-like character. Parts are: head, eyes, face, body, and legs. Figure 20 shows concept composition for a hermit-like character and a reptile-like character. This example aim to demonstrate that our method can learn a large number (i.e., in this case, 7 parts per image) of fine-grained concepts for parts and re-compose them. Parts are: head, eyes, face, nose, arms, body, and legs.

C.2 Cross-category Results

To demonstrate generalization beyond intra-category recomposition, we evaluate our method on cross-category part composition. Figure 21 shows 4 hybrid compositions: a chair and a wheel chair, a gym equipment and a wheel chair, a chair and a bed, and a chair and a gym equipment..

D Further Analysis

Visualization for concept predictor. We visualize the convergence of our concept predictor's segmentation head to demonstrate the

effectiveness of maximizing mutual information. Figure 22 illustrates the comparison of segmentation results from concept predictor and the ground truth masks. The concept predictor gradually converge to predict correct segmentation of the parts, showing the effectiveness our concept predictor design.

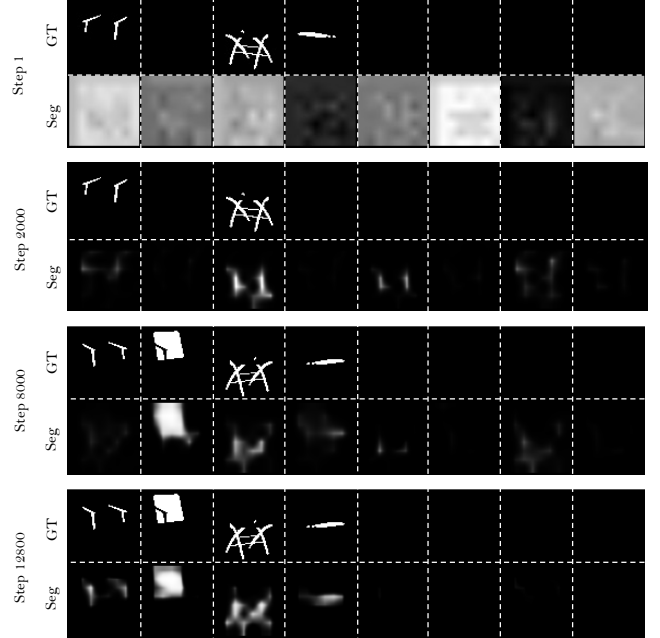


Fig. 22. Visualization for the convergence of segmentation head in our concept predictor.

Weight and Scale Experiments. The most important weight in our experiments is the weight for the concept predictor loss λ_{info} explained in Section 3. We found that $\lambda_{info} = 0.05$ is usually the best weight for most examples, though some examples require slight higher weight ranging from 0.075 to 0.1. Increasing the λ_{info} might show obvious improvement on concept preserving but may result in un-natural artifacts since the diffusion prior may get damaged. Figure 23 illustrates this phenomena. When increasing the weight from 0.01 to 0.05, concepts identity preservation is improved, showing the effectiveness of our concept predictor. When further increasing the weight, although concepts are still well-preserved, there are some visual artifacts including saturation shift.

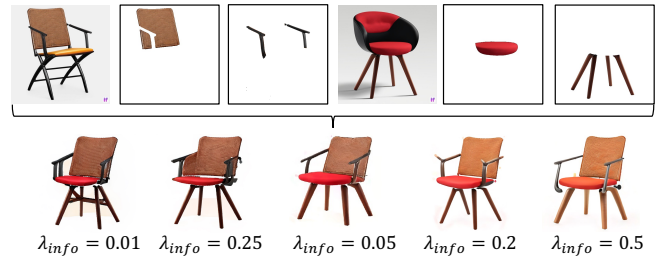


Fig. 23. Visualization of the impacts of different information loss weight



Fig. 11. Concept composition results for various compositions of chair parts.

E Limitations

Although our method can learn well entangled part-level concepts can re-compose them, the image generation quality for some challenging inputs might still need improvement. For example, when composing parts from a truck and a sports car in Figure 15, there are some noticeable artifacts in the generated images even though all the intended part concepts are preserved. Our pipeline also sometimes

do not preserve the exact details for very thing or high-frequency structures like the horizontal bars in chair legs (in Figure 5) and the number of bird legs (in Figure 19). This problem might partially due to the inherent limitation of text-to-image diffusion models since these models can produce images containing unrealistic details like a bird with 3 or more legs. Additionally, for cross-category part re-composition, not all compositions of parts result in meaningful virtual objects. For example, when mixing a chair and a gym

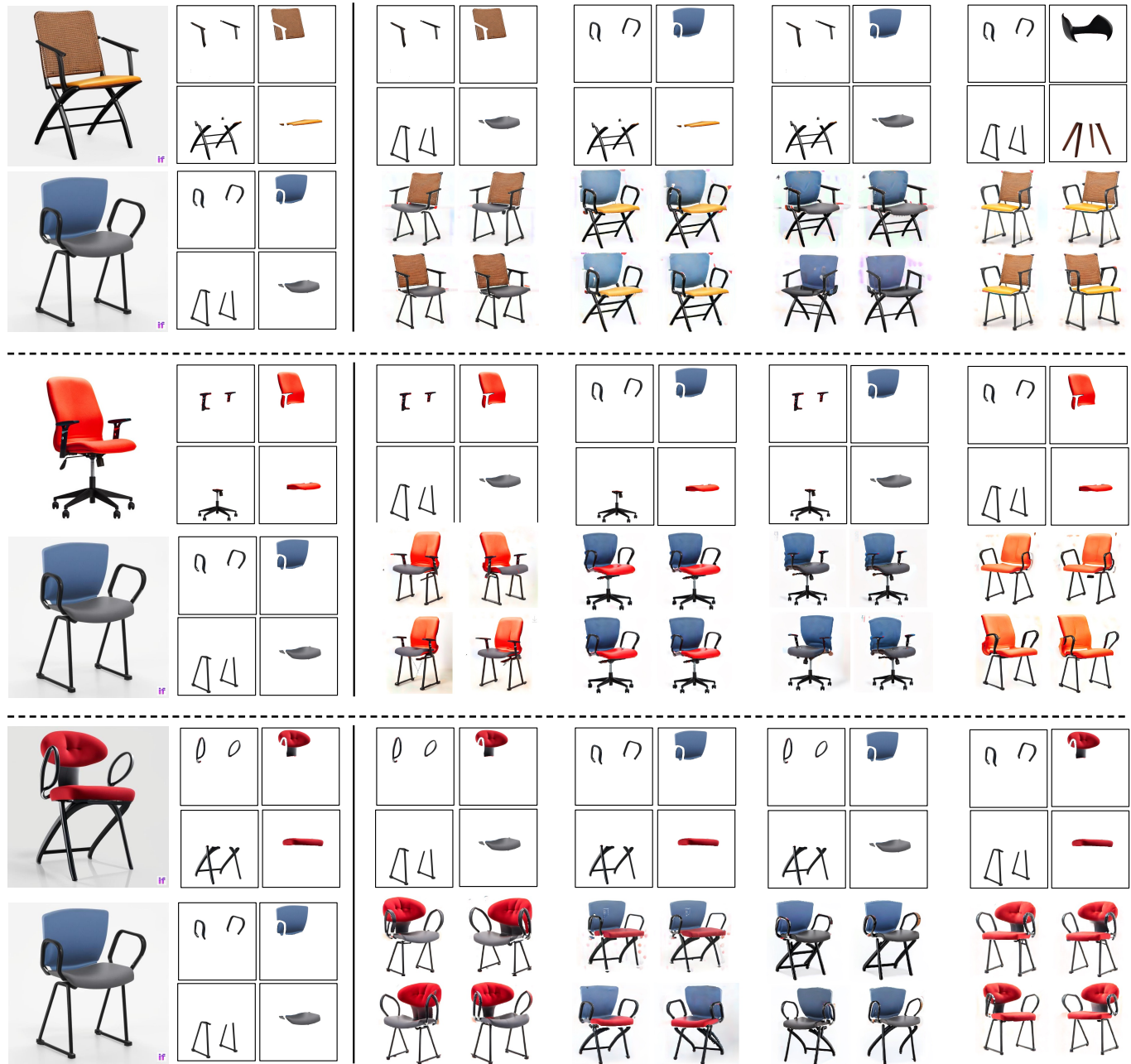


Fig. 12. Concept composition results for various compositions of chair parts.

equipment in Figure 21, the composition in the third column results in non-meaningful objects. A composition prediction scheme may

be developed in this case to predict the possible meaningful part compositions instead of naively trying all possible compositions.

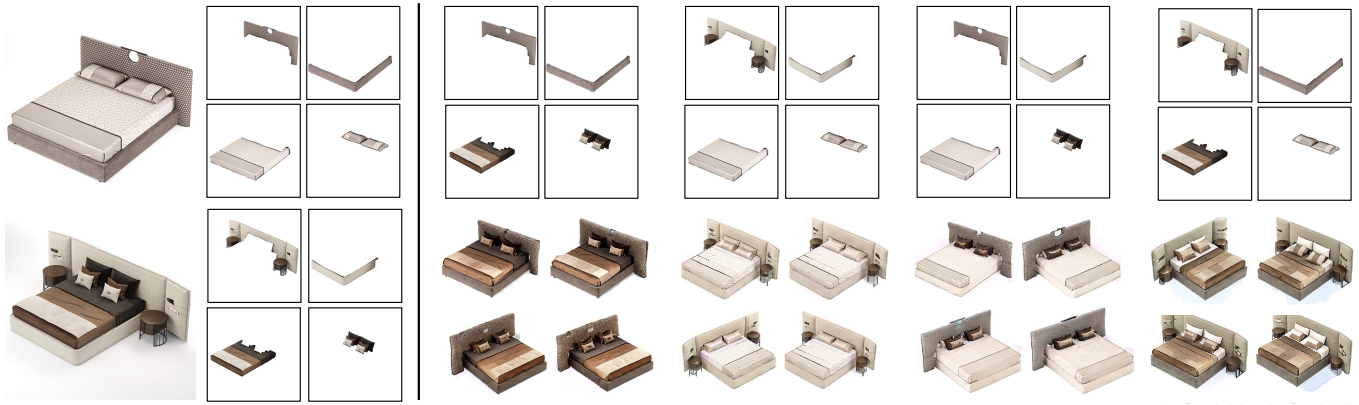


Fig. 13. Concept composition results for beds.

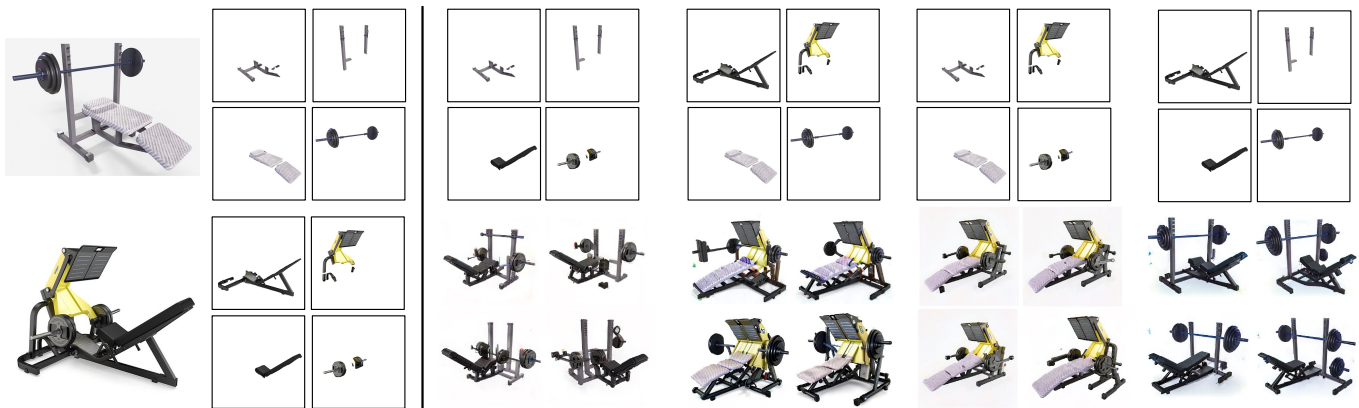


Fig. 14. Concept composition results for gym equipments.



Fig. 15. Concept composition results for vehicles. The first pair contains a sports car and an old formula one car. The second pair contains a sports car and a modern formula one car. The last pair contains a sports car and a truck.

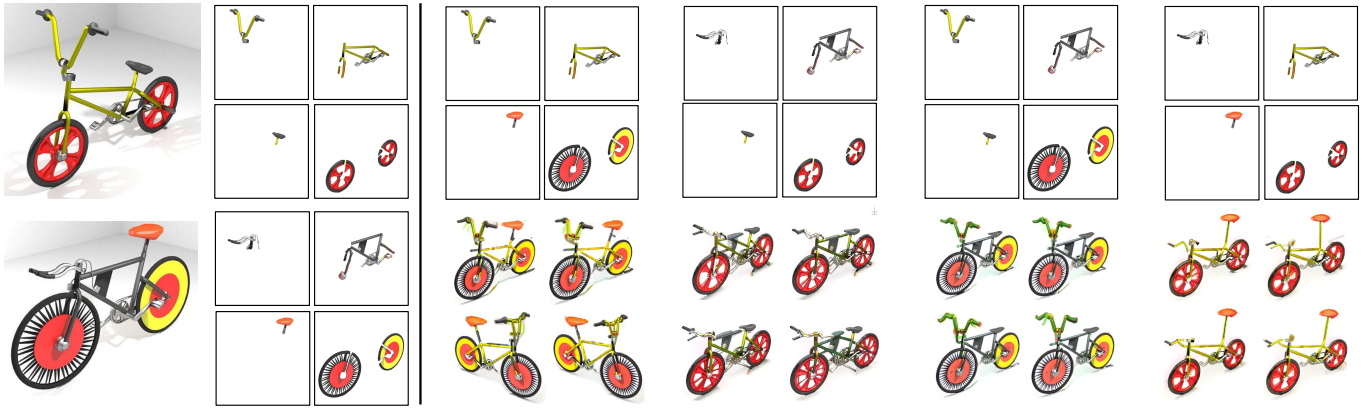


Fig. 16. Concept composition results for bikes.

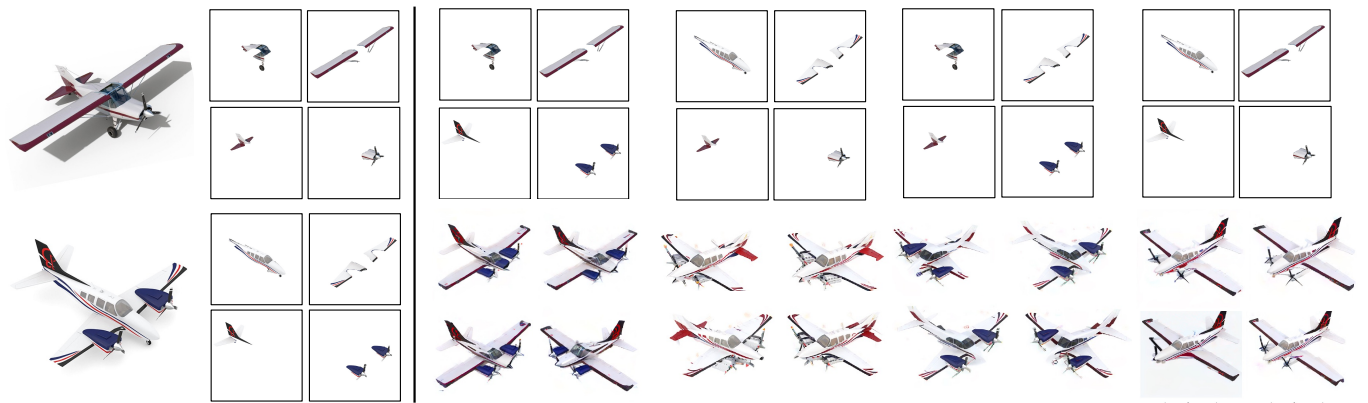


Fig. 17. Concept composition results for planes.



Fig. 18. Concept composition results for robots.

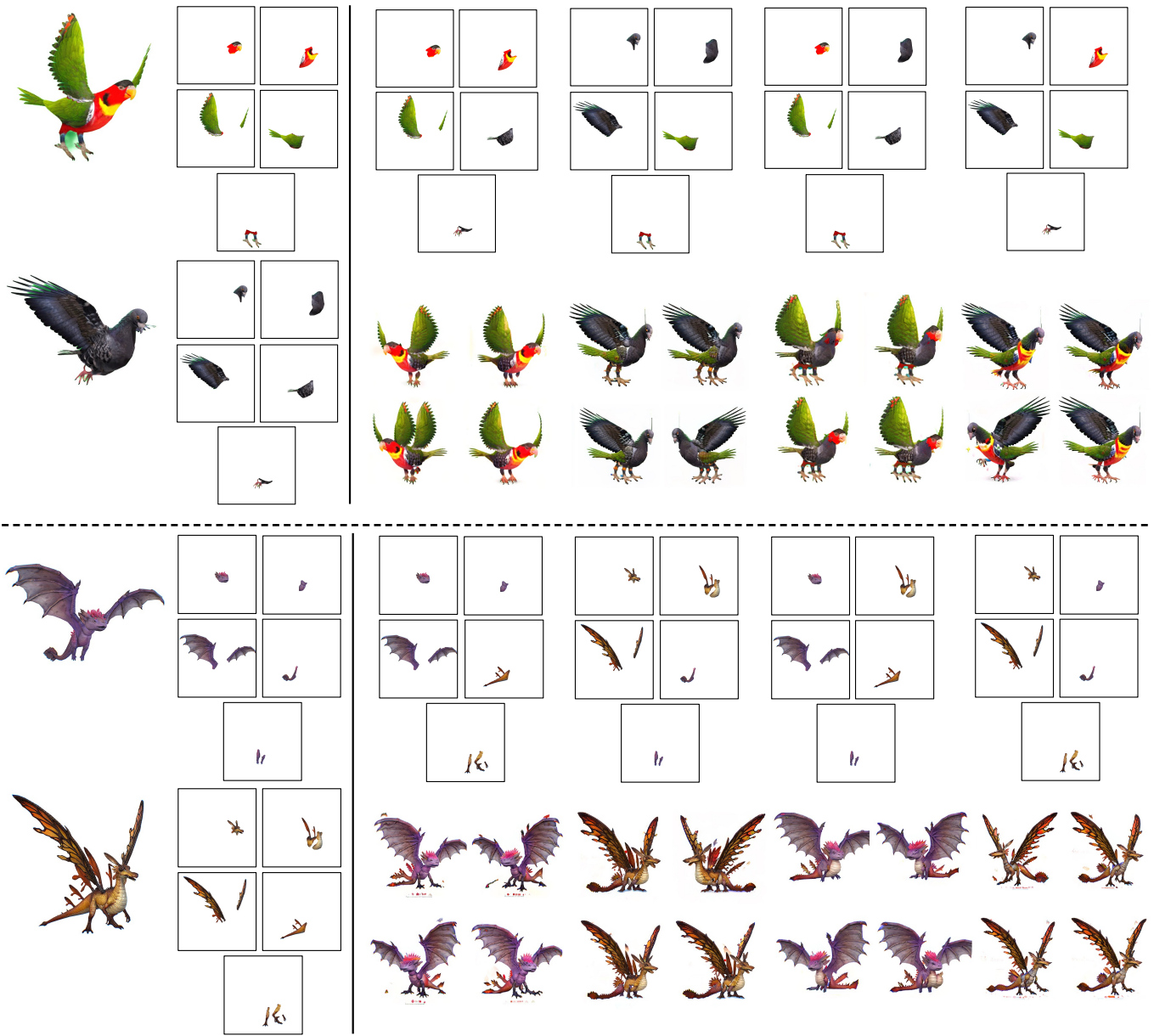


Fig. 19. Concept composition results for birds and dragons.

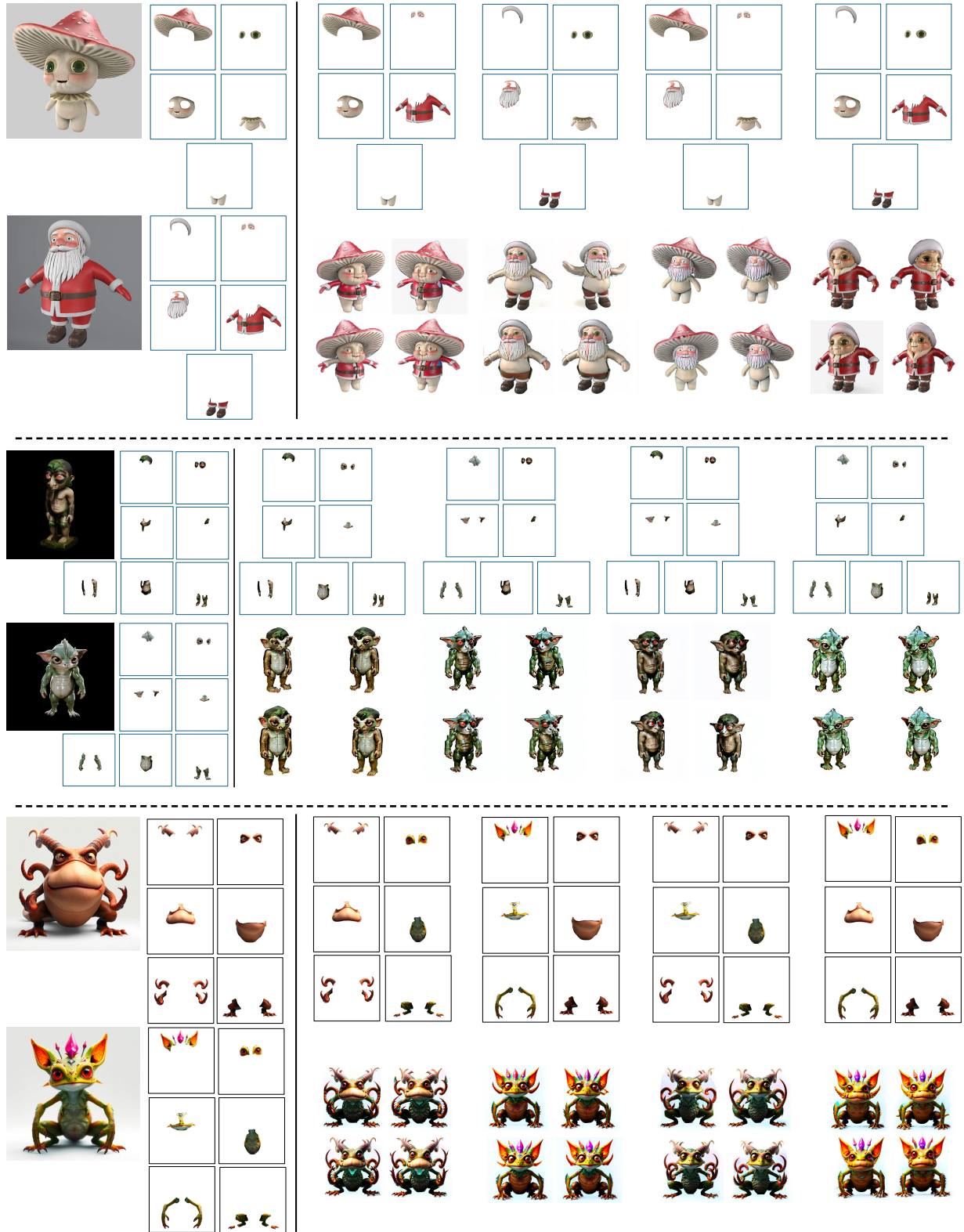


Fig. 20. Concept composition results for virtual creatures: a mushroom-like character and a santa, a hermit and a reptile, and two virtual creatures.

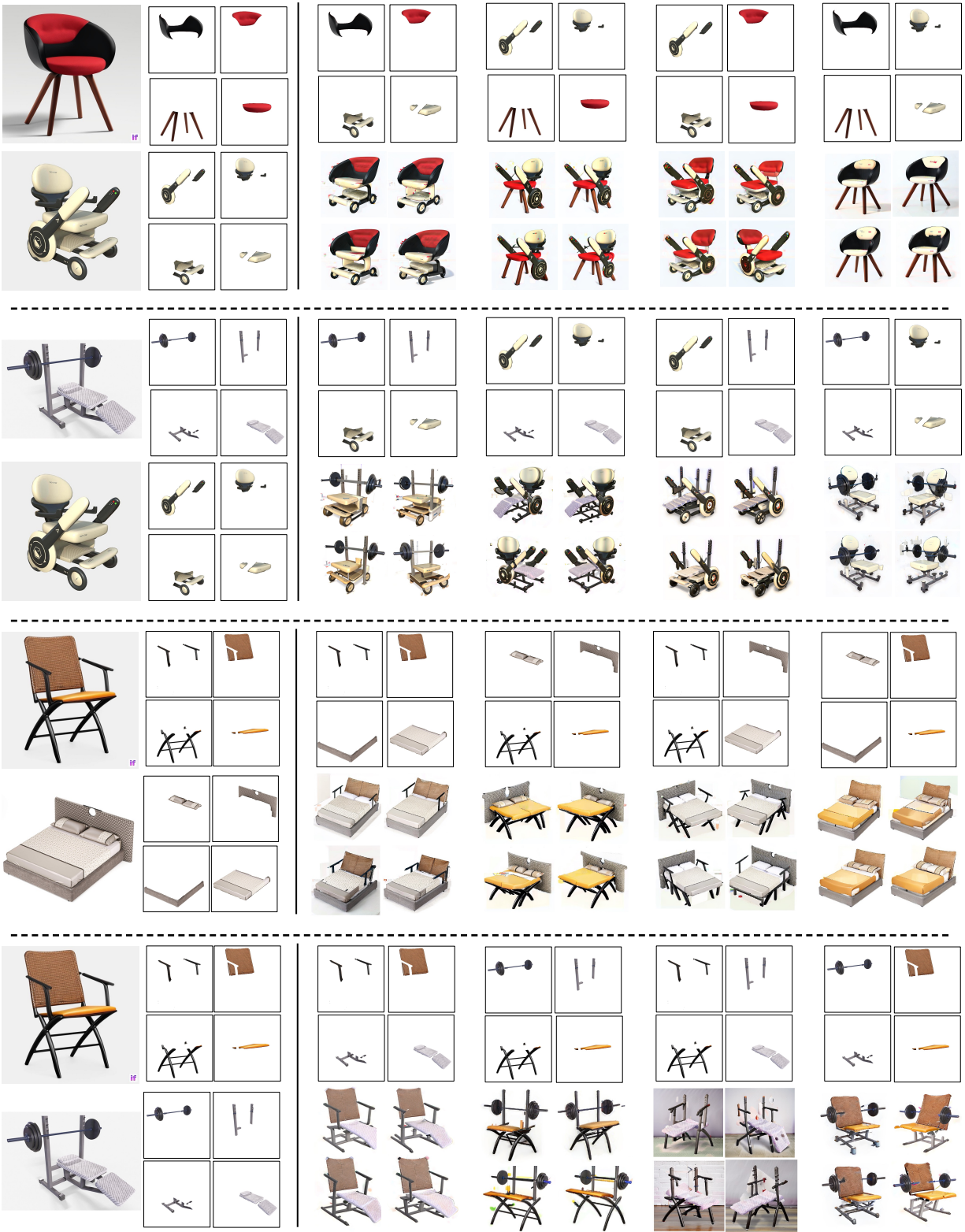


Fig. 21. Concept composition results for cross-category examples: a chair and a wheel chair, a gym equipment and a wheel chair, a chair and a bed, and a chair and a gym equipment.